The reference to the final published version of this paper is:

Berry phase and spin precession without magnetic fields in semiconductor quantum dots, Prabhakar, S. and Melnik, R., EUROPEAN PHYSICAL JOURNAL B, 92 (12), Art. Number: 263, 2019.

DOI: 10.1140/epjb/e2019-100268-3

Berry phase and spin precession without magnetic fields in semiconductor quantum dots

Sanjay Prabhakar[1,2] and Roderick Melnik[2]
[1] *Department of Natural Sciences, Gordon State College, 419 College Drive, Barnesville, GA 30204*

[2] *The MS2Discovery Interdisciplinary Research Institute, M²NeT Laboratory, Wilfrid Laurier University, Waterloo, ON, N2L 3C5 Canada*

(Dated: September 05, 2019)

We investigate electric field control of spin manipulation through Berry phase in III-V semiconductor quantum dots. By utilizing degenerate and non-degenerate perturbation theories, we diagonalize the total Hamiltonian of a semiconductor quantum dot and express the solution of time dependent Schrödinger equation in terms of complete and incomplete elliptic integrals of the second kind, respectively. This allows us to investigate the interplay between the Rashba and Dresselhaus spin-orbit couplings. In particular, we provide theoretical descriptions of several novel properties focusing on spin manipulation through (a) Berry phase, (b) geometric phase and (c) spin echo phenomenon followed by a strong beating patterns during the adiabatic transport of the quantum dots.

I. INTRODUCTION

Several novel ways to trap and manipulate a single electron spin in semiconductor quantum dots with the application of gate potential promise to make next generation spintronic devices for quantum computing and quantum information processing.[1–6] However there are several challenges that need to be overcome before building spintronic devices.[7] A number of research proposals have recently suggested the possibility of using electric field control of single electron spins through spin-orbit coupling in low dimensional semiconductors nanostructures for making non-charge-based logic devices.[8–14] The electric field control of spin-orbit couplings arises from the lack of structural inversion asymmetry originating from the asymmetric triangular quantum well potential along z-direction (Rashba spin-orbit coupling)[15] and the bulk inversion asymmetry (Dresselhaus spin-orbit coupling).[16] The mathematical expressions of spin-orbit couplings, given in Eqs. (9) and (10) later in the paper are widely used in the literature.[17–20] The electric field control of spin-orbit couplings is considered as an essential ingredient for spintronic devices.[17,21–23]

The goal of the present work is to utilize a perturbation scheme to explore the spin splitting behaviors of single electron in very slowly moving quantum dots in a two dimensional plane with no magnetic fields that obey the criteria of adiabaticity. A key result of the present work is the discovery that the quantum dots (QDs) bands may get splitted even in the absence of magnetic fields due to adiabatic movement of the dots in the 2D plane. This allows us investigate a novel idea of the spin manipulation through Berry and geometric phases.[24–26]

A more robust technique can be applied to initialize electron spin states at some phase and read out the states at a different phase by manipulating Berry phase with electric fields in quantum dots.[18,20,23,27,28] For a system of degenerate quantum states, the geometric phase factor is replaced by a non-Abelian time dependent unitary operator acting on the initial states within the subspace of degeneracy that can be further applied to the realization of quantum gates for quantum computing and quantum information processing.[22,29,30] Recent progress in the measurement of the geometric phase for a variety of systems (quantum states driven by a microwave field[31] and qubits with tilted magnetic fields)[32,33] provides an evidence of ongoing research interest for making a solid-state topological quantum computer. Observation of spin echo phenomena is also discussed[34–36]. In this paper, we express the solution of time dependent Schrödinger equation of quantum dots systems in terms of elliptic integrals of the second kind and investigate the interplay between the Rashba and Dreeselhaus spin-orbit couplings on geometric phases. Present innovation is different than our previous work[20] in that even in the presence of applying any source of magnetic fields, the QDs bands may get splitted due to adiabatic movement of the dots in the plane of two dimensional electron gas that still provides a non-vanishing Berry phase and allows us to investigate the interplay between the Rashba and Dresselhaus spin-orbit couplings on the Berry phase.

The paper is organized as follows. In Sec. II, we provide details of the diagonalization technique of total Hamiltonian for a slowly moving quantum dot by utilizing perturbation theory. In Sec. III, we investigate the interplay between the Rashba and Dresselhaus spin-orbit couplings on the Berry phase and geometric phase in III-V semiconductor QDs. Here we also show that the expectation values of Pauli spin matrices behave like in the spin echo phenomena followed by strong beating patterns. We also show that the spin precesses along z-direction which is also the direction of induced intrinsic

magnetic fields due to adiabatic transport of the QDs. Finally, in Sec. IV, we summarize our results.

II. THEORETICAL MODEL

We assume that a semiconductor QD, displaced from the origin ($(x_0, y_0) \neq (0,0)$) in the plane of two-dimensional electron gas, is transported adiabatically with the application of gate controlled electric field. Thus, we write the total Hamiltonian $H = H_0 + H_{so}$ of such quantum dot system as:[17,20,22,23,30,37]

$$H_0 = \frac{p_x^2 + p_y^2}{2m} + \frac{1}{2}m\omega_o^2\left\{(x-x_0)^2 + (y-y_0)^2\right\}, \quad (1)$$

$$H_{so} = \frac{1}{\hbar}\left\{(\alpha p_y - \beta p_x), (-\alpha p_x + \beta p_y), 0\right\}\cdot\sigma. \quad (2)$$

In (1), $\mathbf{p} = -i\hbar(\partial_x, \partial_y, 0)$ is the canonical momentum, m is the effective mass of an electron, $\omega_0 = \hbar/m\ell_0^2$ is the confining potential with ℓ_0 being the QDs radii, $x_0 = r_0\cos\theta$, $y_0 = r_0\sin\theta$ and $\theta = \omega t$. Here r_0 is the orbit radius and ω is the frequency of the control pulse. By varying θ very slowly, QD is adiabatically transported along the circular trajectory in the 2D plane. Eq. (2) is the spin-orbit Hamiltonian consisting of the Rashba and the linear Dresselhaus couplings, where

$$\alpha = \alpha_R eE, \quad (3)$$

$$\beta = 0.78\gamma_c\left(2me/\hbar^2\right)^{2/3}E^{2/3}, \quad (4)$$

and $\sigma = (\sigma_x, \sigma_y, \sigma_z)$ are the 2×2 Pauli spin matrices. Now we assume relative coordinate $\mathbf{R} = \mathbf{r} - \mathbf{r_0} = (X, Y, 0)$ and the relative momentum $\mathbf{P} = \mathbf{p} - \mathbf{p_0} = (P_X, P_Y, 0)$, where $\mathbf{p_0}$ is the momentum of the slowly moving quantum dot that might be classically given by $m\dot{\mathbf{r}}_0$ and formulate the total Hamiltonian H as:

$$H(\mathbf{P},\mathbf{R}) = H_0(\mathbf{P},\mathbf{R}) + H_0'(x_0,y_0) + H_0''(\mathbf{P},\mathbf{R};x_0,y_0) + H_{so}(\mathbf{P},\mathbf{R}) + H_q, \quad (5)$$

$$H_0(\mathbf{P},\mathbf{R}) = \frac{P_X^2 + P_Y^2}{2m} + \frac{1}{2}m\omega_o^2\left(X^2 + Y^2\right), \quad (6)$$

$$H_0'(x_0,y_0) = \frac{1}{2}m\omega^2\left(x_0^2 + y_0^2\right), \quad (7)$$

$$H_0''(\mathbf{P},\mathbf{R};x_0,y_0) = -\omega\left(y_0P_X - x_0P_Y\right), \quad (8)$$

$$H_{so}(\mathbf{P},\mathbf{R}) = \frac{1}{\hbar}\left\{(\alpha P_y - \beta P_x), (-\alpha P_x + \beta P_y), 0\right\}\cdot\sigma, \quad (9)$$

$$H_q(x_0,y_0) = \frac{m\omega}{\hbar}\left\{(\alpha x_0 + \beta y_0), (\alpha y_0 + \beta x_0), 0\right\}\cdot\sigma. \quad (10)$$

For simplicity, we only consider the ground state energy eigenvalues of (6), which is the energy eigen values of quantum dots in relative coordinates system confined in both X and Y directions and then consider H_0', H_0'', H_{so} and H_q as perturbation terms of H_0. Thus we write the eigenenergy as:

$$\varepsilon_{00} = \hbar\omega_0 + \varepsilon_{00}^{(1)} + \varepsilon_{00}^{(2)}, \quad (11)$$

where $\hbar\omega_0$ is the unperturbed energy eigenvalues of H_0. The first order energy corrections are

$$\varepsilon_{00}^{(1)} = \langle 00|H_0' + H_q|00\rangle = G + \frac{m\omega}{\hbar}\left\{\left[\alpha(x_0 - iy_0) + \beta(y_0 - ix_0)\right]\sigma_+ + H.c.\right\}, \quad (12)$$

where $G = m\omega^2 r_0^2/2$ and the second order energy corrections are

$$\varepsilon_{00}^{(2)} = \varepsilon_{00}^{(2)''} + \varepsilon_{00}^{(2)kj} = \sum_{m_+m_- \neq 00}\frac{|\langle m_+m_-|H_0'' + H_{so}|00\rangle|^2}{\varepsilon_{00}^{(0)} - \varepsilon_{m_+m_-}^{(0)}}, \quad (13)$$

where $\varepsilon_{00}^{(2)''}$ and $\varepsilon_{00}^{(2)kj}$ are second order correction terms of H_0'' and H_{so}. For $m_+m_- \neq 00$, we find doubly degenerate states of (6). Thus, we apply degenerate perturbation theory and write

$$\varepsilon_{01}^{(0)} = \varepsilon_{01}^{(0)-} = 2\hbar\omega_0 - G, \quad (14)$$

$$\varepsilon_{10}^{(0)} = \varepsilon_{10}^{(0)+} = 2\hbar\omega_0 + G. \quad (15)$$

Next, we get $\varepsilon_{00}^{(2)''}$ from (13) as:

$$\varepsilon_{00}^{(2)''} = \frac{|\langle 01|H_0''|00\rangle|^2}{\varepsilon_{00}^{(0)} - \varepsilon_{01}^{(0)-}} + \frac{|\langle 10|H_0''|00\rangle|^2}{\varepsilon_{00}^{0} - \varepsilon_{10}^{(0)+}}, \quad (16)$$

$$= -\frac{G(\hbar\omega_0)^2}{(\hbar\omega_0)^2 - G^2}. \quad (17)$$

We also write $\varepsilon_{00}^{(2)kj}$ from (13) as:

$$\varepsilon_{00}^{(2)kj} = \frac{|\langle 01|H_{so}|00\rangle|^2}{\varepsilon_{00}^{0} - \varepsilon_{01}^{(0)-}} + \frac{|\langle 10|H_{so}|00\rangle|^2}{\varepsilon_{00}^{0} - \varepsilon_{10}^{(0)+}}, \quad (18)$$

By considering

$$|\langle 01|H_{so}|00\rangle|^2 = \frac{m\omega_0}{\hbar}\begin{pmatrix}\alpha^2 & 0\\ 0 & \beta^2\end{pmatrix}, \quad (19)$$

$$|\langle 10|H_{so}|00\rangle|^2 = \frac{m\omega_0}{\hbar}\begin{pmatrix}\beta^2 & 0\\ 0 & \alpha^2\end{pmatrix}, \quad (20)$$

we write $\varepsilon_{00}^{(2)kj}$ from (13) as:

$$\varepsilon_{00}^{(2)kj} = \begin{pmatrix}\varepsilon_{00}^{(2)11} & 0\\ 0 & \varepsilon_{00}^{(2)22}\end{pmatrix}, \quad (21)$$

where

$$\varepsilon_{00}^{(2)11} = -\frac{m\omega_0}{\hbar}\left[\frac{\alpha^2}{\hbar\omega_0 - G} + \frac{\beta^2}{\hbar\omega_0 + G}\right], \quad (22)$$

$$\varepsilon_{00}^{(2)22} = -\frac{m\omega_0}{\hbar}\left[\frac{\beta^2}{\hbar\omega_0 - G} + \frac{\alpha^2}{\hbar\omega_0 + G}\right]. \quad (23)$$

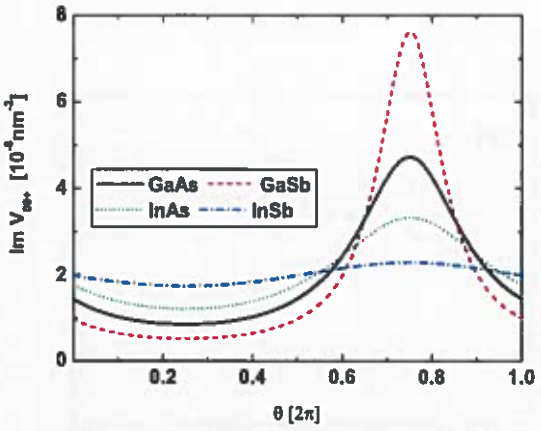

FIG. 1. V_{00+} varies with rotation angle that induces a non-zero Berry phase (see Fig. 2) for topological quantum computing, as an example. Here we chose $r_0 = 500$ nm, $\omega = 100$ GHz and $E = 2\text{x}10^5$ V/cm. Other material constants are chosen from Ref. I.

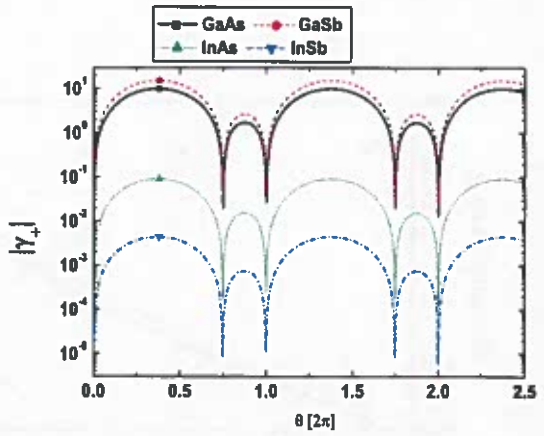

FIG. 2. Geometric phase vs rotation angle in III-V semiconductor quantum dots for symmetrically mixed Rashba-Dresselhaus spin-orbit coupling ($\alpha = \beta$). The materials parameters are chosen as same to Fig. 1.

Finally, substituting the values of $\varepsilon_{00}^{(1)}$ and $\varepsilon_{00}^{(2)}$ in (11), we write the total eigenenergy as:

$$\varepsilon_{00\sigma_z} = (1-\delta)\,\hbar\omega_0 + \sqrt{\kappa}\sigma_z, \tag{24}$$

where $\delta(<1) = (m\omega_0/\hbar)(\alpha^2+\beta^2)/[(\hbar\omega_0)^2 - G^2]$. In (24), we have neglected the term associated to $\tilde{\varepsilon}_{00}^{(2)+}\cdot\tilde{\varepsilon}_{00}^{(2)-} << 1$. Also,

$$\kappa = \left(\frac{m\omega}{\hbar}\right)^2\left[(\alpha x_0 + \beta y_0)^2 + (\alpha y_0 + \beta x_0)^2\right]. \tag{25}$$

From (24), it is also clear that the bandstructures of quantum dots explicitly depend on the adiabatic parameters, x_0 and y_0 and the Rashba-Dresselhaus spin-orbit coupling coefficients. Thus we expect large splitting of QDs bands for the materials that possess large spin-orbit coupling coefficients (e.g. InSb). By varying θ very slowly, we expect resonant behaviors of the energy eigenvalues of QDs bands.

TABLE I. The material constants used in our calculations are taken from Refs. 5

Parameters	GaAs	InAs	*GaSb*	InSb
g_0	-0.44	-15	−7.8	-50.6
m	0.067	0.0239	0.0412	0.0136
γ_R [Å^2]	4.4	110	33	500
γ_D [eVÅ^3]	26	130	187	228
eh_{14} [$10^{-5}erg/cm$]	2.34	0.54	1.5	0.75
s_l [$10^5 cm/s$]	5.14	4.2	4.3	3.69
s_t [$10^5 cm/s$]	3.03	2.35	2.49	2.29
ρ [g/cm^3]	5.3176	5.667	5.6137	5.7747

III. RESULTS AND DISCUSSIONS

From (24), it is clear that the splitting of energy eigenvalue is possible due to the presence of quasi-spin Hamiltonian (10) that originates from the adiabatic movement of the dots in the plane of two dimensional electron gas. Our present work is different from our previous work (Ref. 37) in that we utilized the splitting of the QDs bands to investigate several other properties such as Berry phase, geometric phase and spin precession for applications in spintronic devices. Below we investigate these properties in details.

A. Berry phase

We assume that the relative variables change rapidly while the center of the confining potential moves adiabatically. Thus at any fixed time, the transformed Hamiltonian of QDs gives rise to a static energy spectrum which can be evaluated by perturbation scheme. The effect of adiabatic transport is all contained in the phase of the state vector $|\psi\rangle$. After one completes adiabatic rotation, we may extract all topologically protected quantum information readout data from the Berry phase. The expression for the Berry phase can be evaluated as:[27]

$$\gamma_{00+} = -Im\int_S d\mathbf{S}\cdot\mathbf{V}_{00+}(x_0, y_0), \tag{26}$$

where

$$\mathbf{V}_{00+} = \frac{\langle 00+|\nabla_{x_0,y_0}H|00-\rangle \times \langle 00-|\nabla_{x_0,y_0}H|00+\rangle}{\left[\varepsilon_{00-}(x_0,y_0) - \varepsilon_{00+}(x_0,y_0)\right]^2}. \tag{27}$$

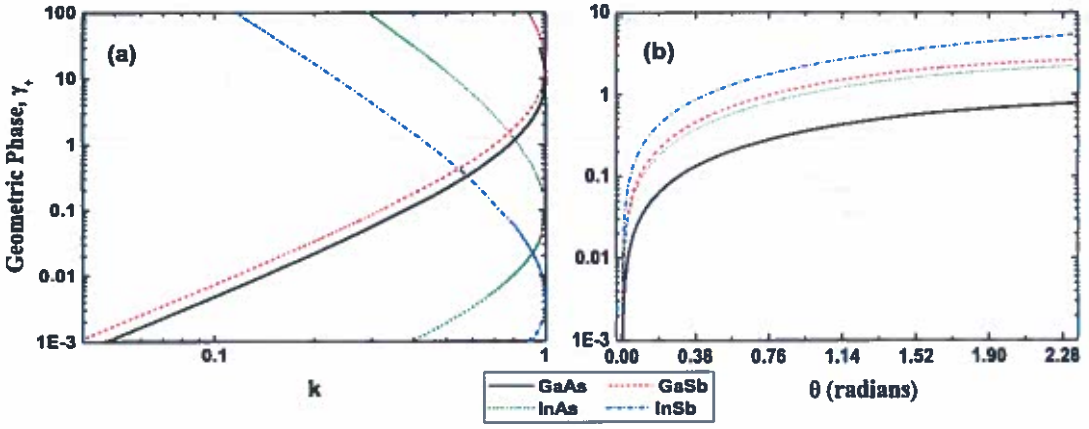

FIG. 3. (a) Geometric phase vs interplay between Rashba-Dresselhaus spin-orbit coupling coefficients, $\tilde{k}\,(\leq 1) = 4\alpha\beta/(\alpha+\beta)^2$. (b) Geometric phase vs θ for $E = 10^5$ V/cm. Here we consider the solution of (41) in terms of complete elliptic integral of the second kind (Fig. 3(a)) and incomplete elliptic integral of the second kind (Fig. 3(b)). The materials parameters are chosen the same as in Fig. 1.

By substituting the energy eigenvalues for the spin states $|00+\rangle$ and $|00-\rangle$ in (27) and taking the cross product of the terms in the numerator of (27), we write,

$$\mathrm{V}_{00+} = 2i\left(\frac{m\omega}{\hbar}\right)^2 \frac{\alpha^2-\beta^2}{a+b\sin(2\theta)}\hat{z}, \tag{28}$$

where

$$a = 4\left(\frac{m\omega r_0}{\hbar}\right)^2\left(\alpha^2+\beta^2\right), \tag{29}$$

$$b = 8\left(\frac{m\omega r_0}{\hbar}\right)^2\alpha\beta. \tag{30}$$

In (27), we have evaluated

$$\langle 00+|\nabla H|00-\rangle = \frac{m\omega}{\hbar}\left\{\hat{x}\,(\alpha-i\beta)+\hat{y}\,(-i\alpha+\beta)\right\} \tag{31}$$

$$\langle 00-|\nabla H|00+\rangle = \frac{m\omega}{\hbar}\left\{\hat{x}\,(\alpha-i\beta)+\hat{y}\,(-i\alpha+\beta)\right\} \tag{32}$$

and then derived Eq. (28). We have plotted V_{00+} of GaAs, GaSb, InAs and InSb vs rotation angle. After one complete rotation, V_{00+} induces a non-zero Berry phase (see below). Since $a > b$, we write the expressions for the Berry phase from (26) as:

$$\gamma_{00+} = \left(\frac{m\omega r_0}{\hbar}\right)^2 \frac{|\beta^2-\alpha^2|}{\sqrt{a^2-b^2}}\left[\tan^{-1}\left(\frac{a\tan\theta+b}{\sqrt{a^2-b^2}}\right)\right]_{\theta=0}^{2\pi}. \tag{33}$$

The quantity inside the square bracket on the right hand side of (33) vanishes if we directly let $\theta = 2\pi$. Thus we divide the square-bracket into three parts as:

$$[\cdot]_{\theta=0}^{2\pi} = \lim_{\epsilon\to 0}\left([\cdot]_0^{\pi/2-\epsilon} + [\cdot]_{\pi/2+\epsilon}^{3\pi/2-\epsilon} + [\cdot]_{3\pi/2+\epsilon}^{2\pi}\right). \tag{34}$$

Notice that $\tan(\pi/2-\epsilon) > 0$ whereas $\tan(\pi/2+\epsilon) < 0$. As a result of this calculation, we can get the non-vanishing Berry phase which can be written as:

$$\gamma_{00\uparrow} = 2\left(\frac{m\omega r_0}{\hbar}\right)^2 \frac{|\beta^2-\alpha^2|}{\sqrt{a^2-b^2}}(2\pi) = \pi. \tag{35}$$

Thus we express geometric phase factor $\exp\{i\gamma_n(S)\} = \exp\{-in\Omega(S)\} = -1$, where $\gamma = \pi = \Omega$. It means, the geometric phase is the flux through the circular trajectory of the intrinsic magnetic fields $B_{in} = \epsilon_0\mu_r\pi r_0\omega E_0/2c^2$ induced by the adiabatical transport of QDs around a cone of semiangle 60^0 that gives $\gamma = \Omega = \pi$ (see Ref. 27 (section 4)).

B. Geometric phase for degenerate states

The above equation for the Berry phase can be applied only to nondegenerate states and for $\beta \neq \alpha$. For degenerate states, we apply the formulation developed by Wilczek and others[22,29,38] who replaced the geometric phase factor by a non-Abelian unitary operator acting on the initial states within the subspace of degeneracy. In other words (from Eq.(24)), we assume that the relative coordinates of an electron in QDs moves rapidly, so that a dynamical phase factor is induced:

$$\Theta_{00\uparrow,\downarrow} = -\frac{1}{\hbar}\int_0^t (1-\delta)\,\hbar\omega_0 dt' = -(1-\delta)\,\omega_0 t, \tag{36}$$

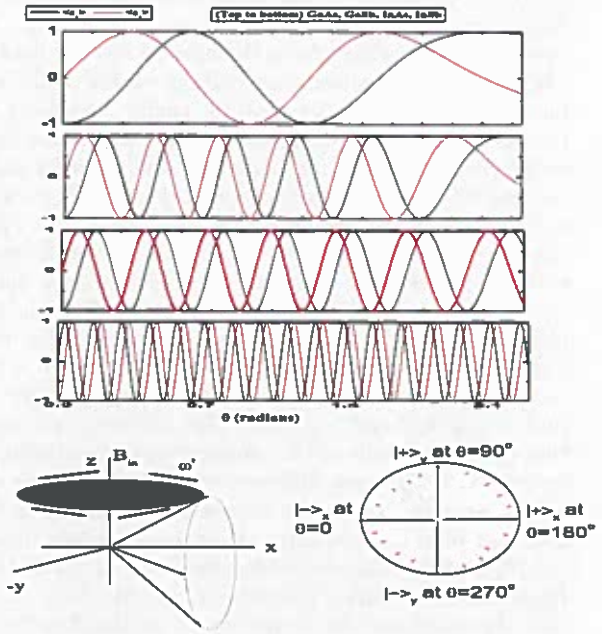

FIG. 4. (Color online) Expectation values of spin matrix, $\langle s_i \rangle$ $(\hbar/2)$(i=x,y) vs rotation angle. We see clearly that periodicity of the propagating waves are different by choosing different materials that are characterized by the strength of the spin-orbit coupling coefficients. The schematics of spin precession (left) and spin echo for GaAs QDs (right) are shown in the lower panel. The materials parameters are chosen the same as in Fig. 1 but $E = 5 \times 10^5$V/cm.

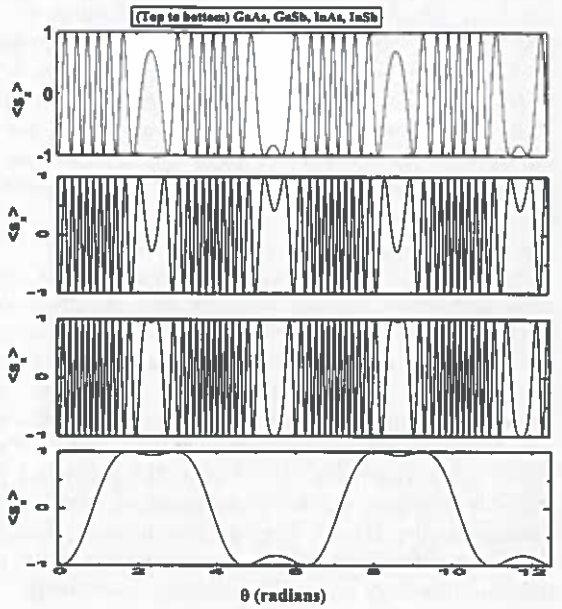

FIG. 5. Expectation values of spin matrix, $\langle s_x \rangle$ $(\hbar/2)$ vs rotation angle for $\alpha = \beta$. The electric field, which is different for different materials, for the equal strength of Rashba and Dresselhaus spin-orbit couplings (i.e., $\alpha = \beta$), is calculated by using Eqs. 3 and 4. In all materials, we find spin waves followed by strong beating patterns. The materials parameters are chosen the same as in Fig. 1 but $r_0 = 100\mu$m for InAs and InSb QDs.

where $\delta(<1) = (m\omega_0/\hbar)(\alpha_R^2 + \alpha_D^2)/[(\hbar\omega_0)^2 - G^2]$. The spin in QDs is considered to be the only degree of freedom that the electron possesses around the induced intrinsic magnetic fields due to the adiabatic movement of the QDs along the circular trajectory that provides the geometric phase:

$$\gamma_\pm = i\int_0^t \langle \chi_\pm(t') | \partial_{t'} \chi_\pm(t') \rangle dt', \tag{37}$$

where the wavefunction $\chi(t) = (\chi_+(t) \;\; \chi_-(t))^T$ can be found by solving the time dependent Schrödinger equation

$$i\hbar \frac{d}{dt}|\chi(t)\rangle = \sqrt{\kappa}\sigma_x|\chi\rangle. \tag{38}$$

We write the solution of (38) as:

$$\chi(t) = \begin{pmatrix} \chi_+(0)e^{\left[-i\left(\frac{mr_0\lambda}{\hbar^2}\right)\left\{E(\phi,\tilde{k})+E\left(\frac{\pi}{4},\tilde{k}\right)\right\}\right]} \\ \chi_-(0)e^{\left[i\left(\frac{mr_0\lambda}{\hbar^2}\right)\left\{E(\phi,\tilde{k})+E\left(\frac{\pi}{4},\tilde{k}\right)\right\}\right]} \end{pmatrix}, \tag{39}$$

where $\chi_+(0)$ and $\chi_-(0)$ are determined by the initial conditions where $|\chi_+(0)|^2 + |\chi_-(0)|^2 = 1$. Throughout this paper, we chose $\chi(0) = (\chi_+(0) \; \chi_-(0))^T = 1/\sqrt{2}\,(1 \;\; -1)^T$. Also $\lambda = \alpha + \beta$ and $E(\phi, \tilde{k})$ is the elliptic integral of 2nd kind which is given by

$$E\left(\phi, \tilde{k}\right) = \int_0^\phi \sqrt{1 - \tilde{k}\sin^2\theta}\; d\theta, \tag{40}$$

where $\phi = \theta - \pi/4$ and $\tilde{k} = 4\alpha\beta/\lambda^2$. Thus we write the geometric phase as:

$$\gamma_\pm = \pm|\chi_\pm(0)|^2 \frac{mr_0\lambda}{\hbar^2}\left\{E\left(\phi,\tilde{k}\right) + E\left(\frac{\pi}{4},\tilde{k}\right)\right\}. \tag{41}$$

For equal strength of Rashba and Dresselhaus spin-orbit couplings ($\alpha = \beta$), we write the exact solution of (41) as:

$$\gamma_\pm = \pm|\chi_\pm(0)|^2 \frac{\sqrt{2}mr_0\alpha}{\hbar^2}\left(|\sin\theta - \cos\theta + 1|\right). \tag{42}$$

In Fig. 2, we have plotted the geometric phase vs rotation angle. Here we find resonant behaviors at fixed time intervals due to the superposition of the spin waves for the mixed Rashba-Dresselhaus spin-orbit couplings. Note that either for the pure Rashba or the pure Dresselhaus case, we do not expect to see the resonant behaviors (see Eq.24). The exact ideal location of the resonant behaviors can be found from the condition

$$\theta_n = (2n+1)\,\pi/2, \quad \theta_m = m\pi, \tag{43}$$

where n is the odd integer and m is the even integer. In Fig. 3(a), we have plotted the geometric phase vs interplay between Rashba-Dresselhaus spin-orbit couplings, $k = 4\alpha\beta/(\alpha+\beta)^2$ by considering the solution of (41) in terms of the complete elliptic integral of the second kind. The numerical values of the geometric phase factor at $\tilde{k} = 1$ is small for InSb due to the fact that the Rashba and Dresselhaus spin-orbit couplings become equal at very low applied electric field $E = 57.3$ V/cm. The enhancement of the geometric phase at $\tilde{k} = 1$ can be seen for GaSb QDs because the Rashba and Dresselhaus spin-orbit couplings become equal at large applied electric field $E = 10^6$ V/cm. In Fig. 3(b), we have plotted the geometric phase vs rotation angle by considering the solution of the geometric phase (41) in terms of the incomplete elliptic integral of the second kind. Evidently that the geometric phase factor vanishes at $\theta = 0$ which is our initial condition. For $\theta \neq 0$, the geometric phase factor is enhanced and is the monotonous function of the rotation angle. Here a large geometric phase factor can be observed for InSb QDs due to the fact that the material contains large spin-orbit coupling coefficients.

C. Spin Precession during adiabatic transport of the QDs

Assume that an electron is localized at a crystal site and then consider that the spin is the only degree of freedom. Thus the spin precession about the z-axis is obtained by finding expectation values of spin matrices as a function of time:

$$\langle s_x\rangle = -\frac{\hbar}{2}\cos\left[\frac{2mr_0\lambda}{\hbar^2}\left\{E(\phi,k)+E\left(\frac{\pi}{4},k\right)\right\}\right]. \quad (44)$$

$$\langle s_y\rangle = -\frac{\hbar}{2}\sin\left[\frac{2mr_0\lambda}{\hbar^2}\left\{E(\phi,k)+E\left(\frac{\pi}{4},k\right)\right\}\right]. \quad (45)$$

For $\alpha = \beta$, we write (44) and (45) as:

$$\langle s_x\rangle = -\frac{\hbar}{2}\cos\left\{\frac{2\sqrt{2}mr_0\alpha}{\hbar^2}|(\sin\theta-\cos\theta+1)|\right\}, \quad (46)$$

$$\langle s_y\rangle = -\frac{\hbar}{2}\sin\left\{\frac{2\sqrt{2}mr_0\alpha}{\hbar^2}|(\sin\theta-\cos\theta+1)|\right\}. \quad (47)$$

Thus, the spin precesses about the z-axis (see schematics of Fig. 4 (left lower panel)), which is also the direction of induced intrinsic magnetic fields, B_{in} due to the adiabatic movement of QDs with frequency $\omega' = 2mr_0\lambda\{E(\phi,k)+E(\pi/4,k)\}/\hbar^2 t$. The induced intrinsic magnetic field can be found as follows. First we evaluate displacement current density, $J_{in} = \epsilon\partial_t E = \epsilon\omega E_0(y_0,-x_0)/r_0$, and then write induced current $I_{in} = \pi r_0^2|J_{in}|$. Finally, we apply Ampere's law to find the induced intrinsic magnetic field at the center of the orbit $B_{in}(\hat{z}) = \epsilon\mu\pi r_0\omega E_0/2$ and at off center point $B_{in}(\hat{x}) = B_{in}(\hat{y}) = 0$. Here we write $\epsilon = \epsilon_0\epsilon_r$, $\mu = u_0\mu_r$ and $r_0 = eE_0/m\omega_0^2$, where E_0 is the applied electric field. In Fig. 4, we have plotted expectation values of the spin matrices, $(\langle s_x\rangle, \langle s_y\rangle)$ vs rotation angle. Evidently the periods of the propagating waves in spin precession is different (i.e., maximum for GaAs and minimum for InSb), because the spin precession frequency depends on spin-orbit coupling coefficients which are different for different materials. For GaAs at $\theta = 0$, the electron is in the state $|-\rangle_x$ and at $\theta = 90^o$, it is in the state $|+\rangle_y$ and so on. Between $\theta = 0$ and 90^o, we observe the spin echo phenomenon which is schematically shown on the right lower panel (red, dotted line). For example, at $\theta = 20^o$, we find $\langle s_x\rangle = 0$ and $\langle s_y\rangle = \hbar/2$, and at $\theta = 36^o$, we find $\langle s_x\rangle = \hbar/2$ and $\langle s_y\rangle = 0$. This confirms once again that the periodicities of the propagating waves during the transport of QDs are different which gives us the spin echo phenomenon that can be clearly seen in Fig. 5.[39] In Fig. 5, we have plotted expectation values of spin matrix, $(\langle s_x(\theta)\rangle)$ vs rotation angle for mixed case of the Rashba-Dresselhaus spin-orbit couplings ($\alpha = \beta$). Here we see that the superposition of spin waves for the Rashba and Dresselhaus spin-orbit couplings induces the spin echo phenomenon followed by strong beating patterns(also see Ref.[39]).

IV. CONCLUSION

To conclude, we have proposed a novel idea to induce large pseudo-Zeeman spin splitting of the QDs bands due to adiabatic movement of the QDs that induces intrinsic magnetic fields. In Figs. 1,2,3, we have shown that the bands splitting of QDs due to induced intrinsic magnetic fields can be applied to manipulate spins through Berry phase and geometric phase. We have shown that the Berry phase is the flux through the circular trajectory of the induced intrinsic magnetic fields around a cone of semiangle 60^0. In Figs. 4 and 5, we have shown that spin precesses around the z-axis and spin echo phenomenon followed by strong beating patterns can be observed for mixed cases of the Rashba-Dresselhaus spin-orbit couplings.

ACKNOWLEDGMENTS

R. M. was supported by the Natural Sciences and Engineering Research Council (NSERC) of Canada, the Canada Research Chair (CRC) program, and the Bizkaia Talent Grant under the Basque Government through the BERC 2014-2017 program, as well as Spanish Ministry of Economy and Competitiveness MINECO: BCAM Severo Ochoa excellence accreditation SEV-2013-0323.

[1] R. de Sousa and S. Das Sarma, Phys. Rev. B **68**, 155330 (2003).
[2] S. Takahashi, R. S. Deacon, K. Yoshida, A. Oiwa, K. Shibata, K. Hirakawa, Y. Tokura, and S. Tarucha, Phys. Rev. Lett. **104**, 246801 (2010).
[3] S. Prabhakar and J. E. Raynolds, Phys. Rev. B **79**, 195307 (2009).
[4] S. Prabhakar, J. E. Raynolds, and R. Melnik, Phys. Rev. B **84**, 155208 (2011).
[5] S. Prabhakar, R. Melnik, and L. L. Bonilla, Phys. Rev. B **87**, 235202 (2013).
[6] D. D. Awschalom, D. Loss, and N. Samarth, *Semiconductor Spintronics and Quantum Computation* (Springer, Berlin, 2002).
[7] D. D. Awschalom and M. E. Flatté, Nature Physics **3**, 153 (2007).
[8] C. Şahin and M. E. Flatté, Physical review letters **114**, 107201 (2015).
[9] J. van Bree, A. Y. Silov, P. Koenraad, and M. Flatté, Physical Review B **90**, 165306 (2014).
[10] J. van Bree, A. Y. Silov, P. Koenraad, and M. Flatté, Physical review letters **112**, 187201 (2014).
[11] V. Kornich, P. Stano, A. A. Zyuzin, and D. Loss, Physical Review B **91**, 195423 (2015).
[12] L. Trifunovic, F. L. Pedrocchi, S. Hoffman, P. Maletinsky, A. Yacoby, and D. Loss, Nature nanotechnology (2015).
[13] S. D. Sarma, E. Hwang, S. Kodiyalam, L. Pfeiffer, and K. West, Physical Review B **91**, 205304 (2015).
[14] A. Pal, E. I. Rashba, and B. I. Halperin, Phys. Rev. B **92**, 125409 (2015).
[15] Y. A. Bychkov and E. I. Rashba, J. Phys. C **17**, 6039 (1984).
[16] G. Dresselhaus, Phys. Rev. **100**, 580 (1955).
[17] Y. Ban, X. Chen, E. Y. Sherman, and J. G. Muga, Phys. Rev. Lett. **109**, 206602 (2012).
[18] T. Čadež, J. H. Jefferson, and A. Ramšak, Phys. Rev. Lett. **112**, 150402 (2014).
[19] E. I. Rashba, Phys. Rev. B **78**, 195302 (2008).
[20] S. Prabhakar, R. Melnik, and L. L. Bonilla, Phys. Rev. B **89**, 245310 (2014).
[21] D. Rainis and D. Loss, Physical Review B **90**, 235415 (2014).
[22] S. Prabhakar, J. Raynolds, A. Inomata, and R. Melnik, Phys. Rev. B **82**, 195306 (2010).
[23] P. San-Jose, G. Zarand, A. Shnirman, and G. Schön, Phys. Rev. Lett. **97**, 076803 (2006).
[24] Z.-Y. Xue, J. Zhou, and Z. D. Wang, Phys. Rev. A **92**, 022320 (2015).
[25] A. W. Cross and J. M. Gambetta, Phys. Rev. A **91**, 032325 (2015).
[26] S.-B. Zheng, Phys. Rev. A **91**, 052117 (2015).
[27] M. V. Berry, Proceedings of the Royal Society of London. Series A, Mathematical and Physical Sciences **392**, 45 (1984).
[28] V. Lopes-Oliveira, L. K. Castelano, G. E. Marques, S. E. Ulloa, and V. Lopez-Richard, Phys. Rev. B **92**, 035441 (2015).
[29] F. Wilczek and A. Zee, Phys. Rev. Lett. **52**, 2111 (1984).
[30] S. Prabhakar, R. Melnik, and A. Inomata, Applied Physics Letters **104**, 142411 (2014).
[31] M. Pechal, S. Berger, A. A. Abdumalikov, J. M. Fink, J. A. Mlynek, L. Steffen, A. Wallraff, and S. Filipp, Phys. Rev. Lett. **108**, 170401 (2012).
[32] S. Berger, M. Pechal, S. Pugnetti, A. A. Abdumalikov, L. Steffen, A. Fedorov, A. Wallraff, and S. Filipp, Phys. Rev. B **85**, 220502 (2012).
[33] P. J. Leek, J. M. Fink, A. Blais, R. Bianchetti, M. Goppl, J. M. Gambetta, D. I. Schuster, L. Frunzio, R. J. Schoelkopf, and A. Wallraff, Science **318**, 1889 (2007).
[34] T. Engl, J. D. Urbina, K. Richter, and P. Schlagheck, Phys. Rev. A **98**, 013630 (2018).
[35] P. Philippopoulos, S. Chesi, J. Salfi, S. Rogge, and W. A. Coish, Phys. Rev. B **100**, 125402 (2019).
[36] E. T. Güldeste and C. Bulutay, Phys. Rev. B **98**, 085202 (2018).
[37] S. Prabhakar and R. Melnik, The European Physical Journal B **88**, 273 (2015).
[38] P. San-Jose, B. Scharfenberger, G. Schön, A. Shnirman, and G. Zarand, Phys. Rev. B **77**, 045305 (2008).
[39] X. J. Wang, S. Chesi, and W. A. Coish, Phys. Rev. Lett. **109**, 237601 (2012).